

Fluorescent Probes

Chromophoric and Dendritic Phosphoramidites Enable Construction of Functional Dendrimers with Exceptional Brightness and Water Solubility

Andrew D. Shaller, Wei Wan, Baoming Zhao, and Alexander D. Q. Li*^[a]

Abstract: The fluorescence brightness of a molecular probe determines whether it can be effectively measured and its water solubility dictates if it can be applied in real-world biological systems. However, molecules brighter than the most efficient fluorescent dyes or particles brighter than quantum dots are hard to come by, especially when they must also be soluble in water. In this report, chromophoric phosphoramidites are used in a solid-state synthesis to construct func-

tional dendrimers. When highly twisted chromophores are chosen and the proper spacers and dendrons are introduced, the resultant dendrimers emit exceptionally bright fluorescence. Chromophores, spacers, and dendrons are stitched together by efficient phosphoramidite reagents, which afford high-yield water-soluble phosphodiester linkages after deprotection. The resulting water-soluble dendrimers are exceptionally bright.

Introduction

Fluorescent imaging probes reveal a wealth of information about molecular mechanisms and biological processes. The key enabling factors are the brightness and water solubility of the probes. Newly designed water-soluble, multi-chromophoric dendrimers offer a promising approach to solve such daunting challenges. Dendrimers are a class of spherical polymers that fill the gap between small molecules and nanoparticles. As such, dendrimers exhibit unique functions that cannot be found in either small molecules or nanoparticles.^[1] Because of the tree-like structures, unlike those of polymeric random coils, spherical dendrimers have been applied in many important areas, including high contrast reagents for magnetic resonance imaging (MRI),^[2] carriers for DNA vectors in gene delivery,^[3] and versatile vehicles for drug delivery.^[4] Indeed, the water-soluble poly(amidoamine) has played an instrumental role in the above nano-biotechnologies.^[5]

Although dendrimers can function both as carrying vehicles and molecular probes, they are not widely used in fluorescence imaging. The reasons include the fact that they are not, thus far, much brighter than organic dyes at the single-molecule level and syntheses of water-soluble, multi-chromophoric dendrimers can be really difficult. A considerable amount of pioneering work has been focused on constructing fluorescent dendrimers (FD) utilizing either flexible or rigid architectures.^[6] Single-molecule fluorescence measurements revealed that per-

ylene-based dendrimers were up to six times brighter than a single fluorophore.^[7] Although various terminal groups promise future aqueous compatibility, water solubility is currently not reported in these rigid dendrimers without the use of detergents.^[8] The progress on water-soluble and non-water-soluble perylene-based polymers has been summarized in recent publications.^[9] A major obstacle encountered in the tightly spaced dendrimers is fluorescence self-quenching, resulting in limited dendrimer brightness in aqueous systems.

We report the first successful use of solid-phase synthesis to construct dendrimers by using the strategy of attenuating surface reactive sites. The linchpin, which was not realized before, is that dendritic growth is prohibited when there are too many growing chains crowded on the solid phase.

Previously, phosphoramidites of fluorophores (F1) based on planar perylene building blocks were synthesized (Scheme 1).^[10] These phosphoramidite reagents are too reactive and suffer self-degradation because the phosphorus atom is attached to the primary alcohol. Moreover, the resultant multi-chromophoric polymers had low fluorescence quantum yields owing to π -stacking. Herein, new phosphoramidites of fluorophores, which use a secondary alcohol and have an asymmetric structure (F2 and F3 in Scheme 1 and 2), are used to solve these challenges. The net results are that both water-soluble and exceptionally bright dendrimers are constructed.

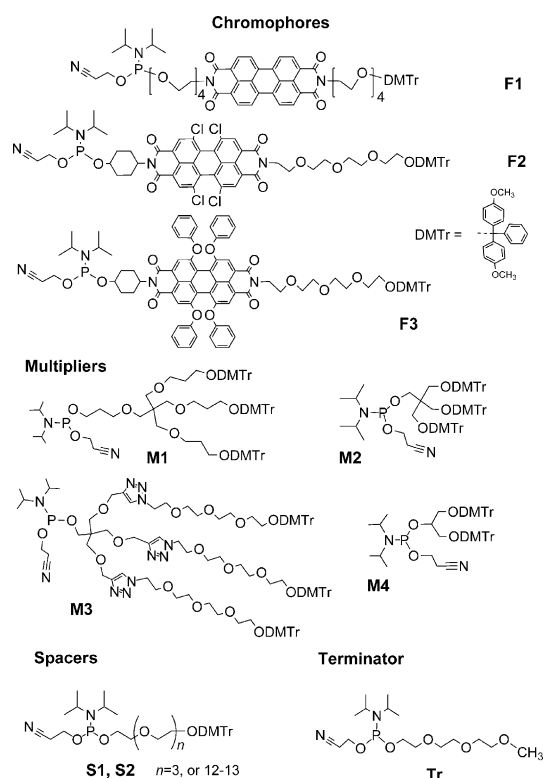
Results and Discussion

In the new chromophoric phosphoramidites, a rigid cyclohexanol amide was used to replace one of the two flexible tetraethylene glycol (TEG) chains for the following important reasons (F2 and F3; also see the Supporting Information, Scheme S1). First, the more sterically demanding cyclohexanol group prevents efficient π -stacking, thus enhancing the bright-

[a] Dr. A. D. Shaller, W. Wan, B. Zhao, Prof. A. D. Q. Li

Department of Chemistry
Washington State University
Pullman, WA 99164 (USA)
E-mail: dequan@wsu.edu

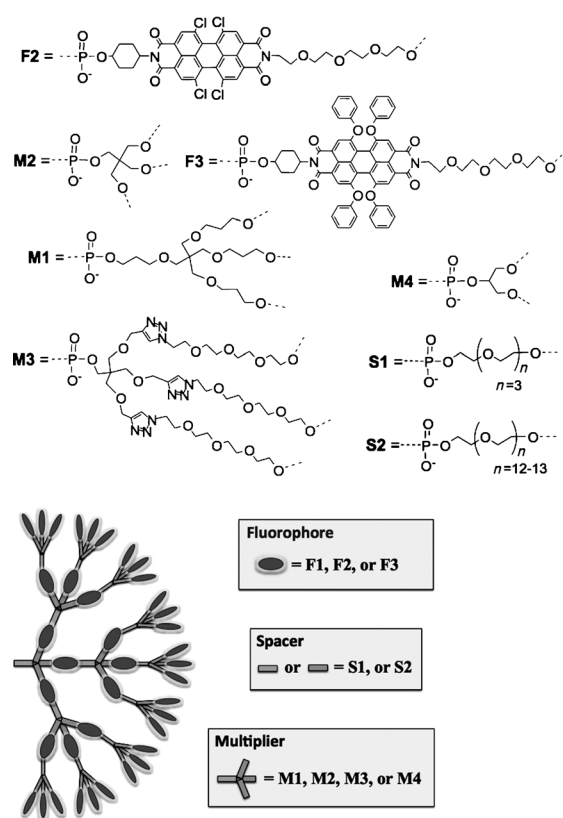
Supporting information for this article is available on the WWW under <http://dx.doi.org/10.1002/chem.201403445>.



Scheme 1. Chemical structures of chromophoric phosphoramidites, dendritic phosphoramidites, spacers, and terminator phosphoramidites used to construct dendrimers on solid supports.

ness of the dendrimers constructed by using such moieties. Similar approaches to the suppression of π - π interactions by using extended spacers have been reported.^[11] Second, the rigidity and the negative charges of the phosphodiester steers the chromophores away from each other, thus greatly suppressing self-quenching and improving fluorescent quantum yields. This point is supported by the fact that perylene diimides functionalized with charged groups have improved aqueous fluorescence quantum yields.^[12] Third, the cyclohexanol amide provides a secondary alcohol for phosphitylation, resulting in a more stable phosphoramidite than that from a primary alcohol. Fourth, the new chromophores are highly twisted, further frustrating π - π stacking and self-quenching. Phosphoramidites from primary alcohols are known for their high reactivity and should be used immediately, within days for better results. In contrast, phosphoramidites from secondary alcohols are rather stable in the solid state and can be stored for later use. The reason that **F2** was chosen as the dendritic building block is that it has a large extinction coefficient ($\epsilon = 4 \times 10^4 \text{ M}^{-1} \text{ cm}^{-1}$)^[13] and near unity quantum yield (ϕ_f).

Complementary to the highly twisted fluorophores, dendritic multipliers based on phosphoramidite chemistry are required for solid-state dendrimer syntheses. Thus, several phosphoramidite multipliers were synthesized (**M1**, **M2**, **M3**, and **M4** in Schemes 1 and 2): a pentaerythritol-based trebler, **M1**, with four propyl branching arms; a short pentaerythritol trebler **M2**; a pentaerythritol-triazole-based trebler **M3**; and a glycerol based doubler **M4** (see the Supporting Information Schem-



Scheme 2. Chemical structures of the various dendrimer building blocks and a schematic illustration of the dendrimer structure. See Table 1 for the dendrimer sequences.

es **S2**–**S5** for details). The hydroxyl groups on **M1** coupled quantitatively at the 5'-end, but this phosphoramidite multiplier did not couple well at the 3'-end, giving "stable" trityl yields,^[14] rather than exponential trityl yields. Adopted from DNA nomenclature, the 5'-end is the dimethoxy trityl (DMTr) terminal; the 3'-end, the phosphoramidite terminal. Short trebler **M2** and doubler **M4** gave higher 3'-coupling yields, but only had 5'-coupling yields around 80%; the likely cause of this lower yield is the close proximity of the terminal hydroxyl groups. Amazingly, the triazole-based trebler (**M3**) shown in Scheme 1 gave excellent tripling yields despite the short linkage to the branching center. The resultant tripling yields as reported by the absorbance of the DMTr group are 275%, or $\geq 91\%$ coupling efficiency, at the root of the phosphoramidite. The terminal hydroxyl groups of the three dendrites are sufficiently far away from each other, enabling nearly quantitative coupling at the 5'-ends, comparable with the coupling efficiency of the standard DNA bases.

Multi-chromophoric dendrimer syntheses were carried out on solid-state supports by alternating the coupling of chromophoric phosphoramidite and trebler phosphoramidite to achieve dendritic growth. Where needed, spacers (**S1** and **S2** in Schemes 1 and 2; also see the Supporting Information, Scheme S6) were introduced to decouple unfavorable molecular interactions that cause fluorescence self-quenching. One advantage of using solid-state synthesis is that it offers rapid

purification. The solid phase can be separated from the complex liquid mixture easily and the dendrimers anchored on the solid supports are pure after a few rinses. Another advantage of using the phosphoramidite approach is high-yield coupling with a reporter trityl group that allows facile monitoring and reporting of the reaction yield for each generation because removing the protecting DMTr groups yields quantitative measures of the growing chains.

After many trial-and-error attempts, an important prerequisite for solid-supported dendrimer synthesis was discovered—the active sites on the commercial CPG (control porous glass) must be first “attenuated” in order to create adequate spacing for dendritic growth later. Without attenuation, trityl yields from previous dendrimer synthesis remained “stable” and no exponential or dendritic growth occurred.^[14] Two attenuation techniques were tested: the first method used a mixture of phosphoramidite terminator **Tr** (Scheme 1, also see the Supporting Information, Scheme S6) with a spacer phosphoramidite **S1** or **S2**, whereas the second method limited the reaction of the spacer **S2** only. A 2:1 ratio of **Tr/S1** was found to work the best and trityl analysis reported that this attenuation consistently killed ~75% of the growing chains in each reactive sequence (Figure 1). Furthermore, the monomethoxy terminator (**Tr**) likely acts as a “comb” to keep the functional ethylene glycol chains optimally extended for the next coupling step.

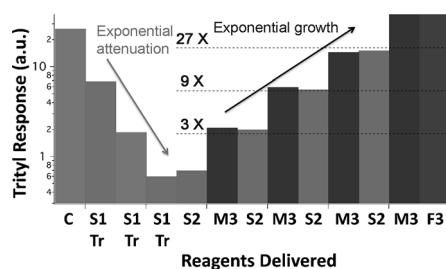


Figure 1. On porous glass spheres, the growing chains were attenuated by using a mixture of **S1** and **Tr** at 1:2 ratio to create space for dendritic growth later. After three attenuation steps, dendrimer synthesis started with the **S2** phosphoramidite to extend the chain and the **M3** trebler to branch the chain. Each tripling step yields the trityl responses on a log scale of nearly ~300%, indicating the anticipated exponential growth of the dendrites. Chemical structures of the dendrimer building blocks are given in Schemes 1 and 2.

Such attenuation creates the necessary space needed for the exponential growth of dendrimers on surfaces.

Following a few steps of attenuation, dendritic growth started by coupling the phosphoramidite to the spacers, chromophores, or treblers (Scheme 2). Figure 1 depicts that coupling efficiency is manifested by the stepwise change in the trityl response. The coupling yields for linear growth, such as attaching spacers or chromophores to the growing chains, were basically quantitative. The average response increased by ~270–280% (compared with 300% in ideal reactions) for each trebling step, indicating ~92% coupling efficiency for attaching the trebler to its root (from **S2** to **S2M3** in Figure 1). Subsequent dendritic growth gave the same near-quantitative coupling of a trebler to the growing chains; this quantitative coupling again resulted in near 270–300% trityl yields after the trebler reaction as shown in Figure 1.

The attenuation and exponential growth strategy worked well and we used it to synthesize dendrimers **D1**–**D8**, depicted in Table 1. The first-generation dendrimer **D1** has a dendritic sequence of **[A-S2-F2-M3≡(F2-S2)₃]**; the second-generation dendrimer **D2** has a dendritic sequence of **[C-S1-S1-S2-M3≡(F2-M3≡(F2-S2)₃)₃]**; the fourth generation dendrimers **D6** and **D7** have dendritic sequences of **[T-S2-S2-S2-S2-S2-M3≡(F2-M3≡(F2-M3≡(F2-ACGT)₃)₃)₃]** and **[T-S2-S2-S2-S2-S2-S2-M3≡(F2-S1-M3≡(F2-S1-M3≡(F2-S1-M3≡(F2-S1-ACGT)₃)₃)₃)₃]**, respectively. Spacers, chromophores and multipliers are defined in Scheme 2; A, T, C, and G stand for regular DNA bases. The automated solid-state synthesizer generates a dendrimer in a few hours, much superior to manual dendrimer syntheses. Once the dendrimer synthesis was completed, concentrated $\text{NH}_4\text{OH}_{(\text{aq})}$ simultaneously cleaved the dendrimers from the solid support and converted the phosphotriester linkages resulting from the phosphoramidite coupling to negatively charged phosphodiester linkages in the dendritic branches make the resultant dendrimer rather soluble in water.

Matrix-assisted laser desorption ionization (MALDI) mass spectrometry was able to confirm the mass of dendrimer **D1**, giving an observed mass of $m/z=7597$, which agrees with the calculated mass of 7597 ($\text{C}_{312}\text{H}_{425}\text{Cl}_{16}\text{N}_{22}\text{O}_{137}\text{P}_{10}\text{Na}_2$). Ensemble optical properties of dendrimers were also collected before single-molecule measurements. Absorption and fluorescence spectra for dendrimers **D2** and **D8** are shown in Figure 2a and

Table 1. Dendrimer sequences along with brightness and diameter.

Dendrimer	Dendritic sequence	Brightness ^[a]	N ^[b]	Diameter ^[c] [nm]
D1	A S2 F2 M3 (F2 S2)₃	2.1	0.53	–
D2	C (S1)₂ S2 M3 (F2 M3(F2 S2)₃)₃	3.9	0.33	12
D3	T (S2)₄ M4 (S2 F2 M4(S2 F2 M4(S2 F2 M4(S2 F2 S2)₃)₃)₃)₃	6.8	0.23	–
D4	T (S2)₃ M3 (F2 M3(F2 M3(F2 ACTG)₃)₃)₃	7.5	0.19	9
D5	N (S2)₃ M3 (F2 S2 M3(F2 S2 M3(F2 S2)₃)₃)₃	20	0.51	10
D6	T (S2)₅ M3 (F2 M3(F2 M3(F2 M3(F2 ACTG)₃)₃)₃)₃	18	0.15	12
D7	T (S2)₆ M3 (F2 S1 M3(F2 S1 M3(F2 S1 M3(F2 S1 ACTG)₃)₃)₃)₃	74	0.62	16
D8	T (S2)₅ M3 (F2 M3(F2 M3(F2 M3(F2 M3(F2 M3(F2 M3(F2 M3(F2 ACTG)₃)₃)₃)₃)₃)₃)₃	114	0.012	12

[a] Modal brightness of dendrimers is determined by using the single-molecule modal brightness as the unit, i.e., the modal intensity of fluorescein or tetra-chloro perylene diimide. [b] Normalized brightness per dye. [c] Diameters of the dendrimers in nanometers are measured using dynamic light scattering.

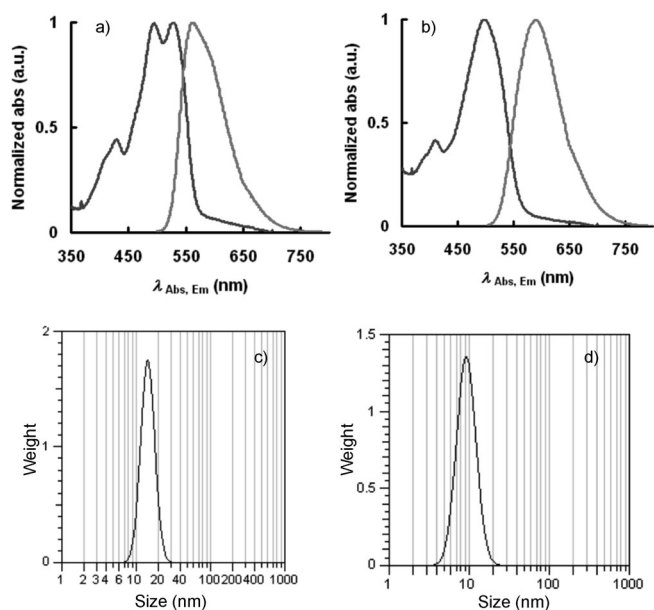


Figure 2. Absorption (left) and fluorescence (right) spectra of dendrimers: a) **D2** and b) **D8** theoretically containing up to 12 and 9840 **F2** fluorophores, respectively. Dynamic light scattering results for c) **D4** and d) **D5** report hydrodynamic diameters that are much smaller than the fully elongated molecular length or even as predicted by the freely jointed chain model.

b. The spectra are similar to the monomer spectra in CH_2Cl_2 except they tend to be broadened and there are varying degrees of intensity reversal between the A^{0-1}/A^{0-0} and F^{0-1}/F^{0-0} vibronic bands, an indication of hydrophobically driven π -stacking, to some degree, between some of the twisted tetrachloro perylene diimides. The A^{0-0}/A^{0-1} ratio changes from dendrimer to dendrimer, and there is not enough data yet to determine a clear trend. The experimental extinction coefficient per chromophore in the dendrimers is $\geq 7 \times 10^3 \text{ M}^{-1} \text{ cm}^{-1}$ because interior and exterior dyes are likely to have different absorption properties depending on generation number, G , fluorophore spacing, and surface groups.

Dynamic light scattering (DLS) measures hydrodynamic diameters of 9–16 nm for these water-soluble dendrimers as shown in Table 1, and Figure 2c and d. These values are smaller than the maximum fully elongated radius of the dendrimers (sequential sum of the segment lengths determined by molecular modelling, for example 10 nm for **D1** to 47 nm for **D8**), whereas the freely jointed chain (FJC) model predicts radii from 6 to 38 nm.^[15] Unlike quantum dots (QDs) or fluorescent nanoparticles that have strong Tyndall effects,^[16] these low-density polyethylene glycol (PEG)-based dendrimers do not scatter light very much, and thus enhancing fluorescence collection efficiency.

The fluorescent quantum yields, ϕ_{fl} , for dendrimers **D1–D8** range between 2% and 24%. Similar to single-molecule brightness, dendrimers with greater intramolecular spacing tend to have higher ϕ_{fl} values. Also, for generations 2–4, ϕ_{fl} appears to decrease with increasing G . Interestingly, for the 8th generation dendrimer **D8**, where hydrophobic encapsulation is likely, ϕ_{fl} rebounds to 20%.

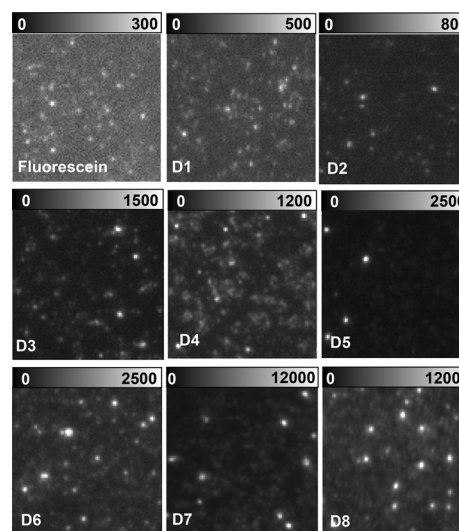


Figure 3. CCD images reveal that dendrimers **D1–D8** are much brighter than single-molecules fluorescein dyes. Note the scale bar differences.

The brightness of these dendrimers were determined by using a home-built single-molecule microscope equipped with a liquid- N_2 cooled CCD and a 488 nm Ar ion laser and two avalanche photodiodes (APDs). The water-soluble dendrimers were uniformly sprinkled on a coverslip so that a single dendrimer could be imaged in the wide field by using either CCD or APD raster scanning.^[17] Figure 3 reveals the representative $10 \times 10 \mu\text{m}$ CCD images with 2 s integration. Fluorescein and 1,6,7,12-tetrachloro perylene diimide (**1e**; see the Supporting Information, Scheme S1) were used to establish the brightness of a single molecule; both had modal brightness of 125 cps (counts per second) under the experimental conditions. The scale bar at the top of each image calibrates the relative brightness intensity, and the modal brightness of dendrimers **D1** and **D2** is 250 and 500 cps, respectively. Thus, the first-generation dendrimer **D1** ($\phi_{\text{fl}} \geq 24\%$) that contains four fluorophores is about twice as bright as the highly fluorescent fluorescein as indicated by the scale bar (Figure 3). Progressively, the second-generation dendrimer **D2** ($\phi_{\text{fl}} \geq 8\%$), which contains up to 12 dyes theoretically, is ~ 4 times brighter than the standard dye fluorescein (Figure 3). Although fluorescence self-quenching still exists in these dendrimers, they are much brighter than previous multi-chromophoric oligomers using planar chromophore **F1** owing to the reasons stated above.^[12]

The fourth-generation dendrimer **D6** ($\phi_{\text{fl}} \geq 4\%$), which contains up to 120 fluorophores and has a modal brightness of 2250 cps, is ~ 18 times brighter than the modal brightness of highly fluorescent fluorescein (125 cps) (Figures 3 and 4). Such dendrimers are as bright as QDs, which have been characterized as 10–20 times as bright as the most efficient fluorescent dyes.^[18] However, the brightness per fluorophore within the dendrimer for this fourth-generation dendrimer is apparently not as high as those of the first- or second-generation dendrimers (**D1** or **D2**). Thus, further potential brightness gain can be realized in the fourth-generation dendrimer if its structure is optimized to further reduce self-quenching and improve

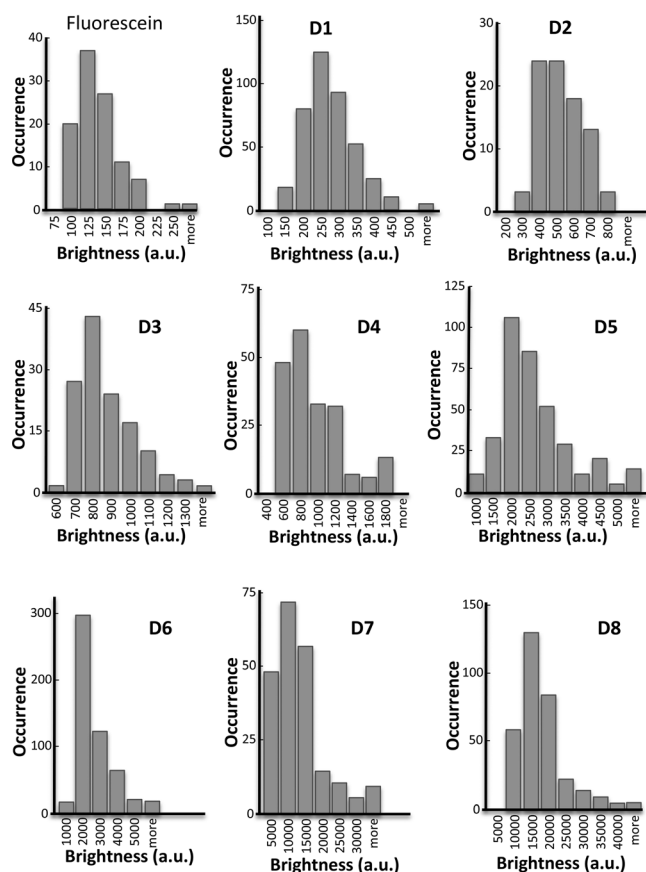


Figure 4. Intensity histograms reveal that fluorescein peaks at 125 cps, whereas the dendrimer **D7** reaches a maximum at 10 000 cps, a near 80 times enhancement in brightness. Other dendrimers are also brighter than the high-quantum-yield dye fluorescein.

quantum yields. Promisingly, increasing the fluorophore spacing has been shown to augment fluorescent intensity.^[19] When a TEG spacer was introduced between **F2** chromophores, the single-molecule fluorescence of the derivatized fourth-generation dendrimer **D7** ($\phi_{fl} \geq 7\%$), with a 16 nm hydrodynamic diameter, has a modal brightness of 10^4 cps, 74 times brighter than a single fluorophore (Figures 3 and 4). Individual QDs seem to have reached a fundamental ceiling at 20 times brighter than single-molecule fluorophores, but dendrimers, which have the molar mass equivalent to 5 nm QDs, can deliver much brighter intensity than the ceiling brightness of QDs.

Time-dependent fluorescence trajectories from single dendrimers were monitored by using diffraction-limited excitation, and representative traces for each generation are shown in Figure 5. Upon shutter opening, a single molecule having the tetrachloro perylene diimide skeleton typically exhibits discreet on–off photoblinking, with eventual photobleaching to the background noise level before shutter closing (Figure 5: **1 e**). In contrast, first-generation **D1**, with four dye units, exhibits at least four discreet photo-blinking or photobleaching steps. With increasing generation number, the number of apparent steps increases until **D8** ($G=8$), which approaches a smooth decay. Interestingly, the size of the step decreases and initial intensity increases sub-linearly with increasing G , suggesting

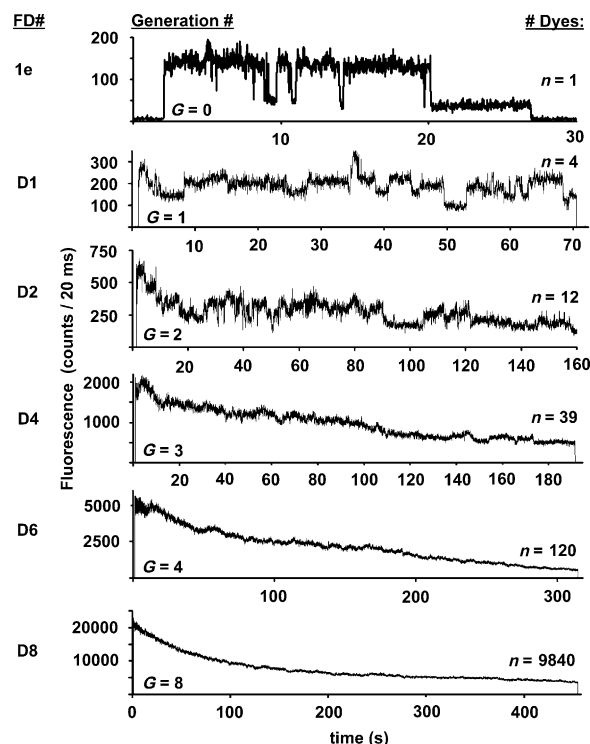


Figure 5. Time traces for dense dendrimers **D1**, **D2**, **D4**, **D6**, and **D8** are compared with a single dye—tetrachloro perylene diimide (**1 e**, see the Supporting Information, Scheme S1). Although a single molecule typically shows one-step on–off blinking before photobleaching, **D1** typically shows four or less discreet steps. Higher generation dendrimers show increasing numbers of smaller bleaching steps and increased overall lifetime. As a result, the trajectories change from stepwise for lower generation dendrimers to continuous for higher generation of dendrimers.

that individual dyes are less bright in the larger dendrimers, consistent with relatively lower quantum yields discussed above. Similar to fluorescent nanoparticles and in contrast to QDs, fluorescent dendrimers do not completely blink on and off. Dendrimer brightness is affected by individual dye photobleaching, photoblinking, and typically exhibits exponential decay where higher generation dendrimers exhibit longer decay lifetimes.

The big picture is that these fluorescent dendrimers have hydrodynamic diameters, as determined by DLS, similar to functionalized QDs and smaller than fluorescent nanoparticles, with similar or higher fluorescent intensity.^[20] Fluorescent dendrimers are smaller than fluorescent polymers or silica nanoparticles but can achieve similar brightness at smaller sizes. This is because dendrimers allow packing of the maximum density of fluorophores into the smallest space with controlled intramolecular fluorophore spacing.

Conclusion

Exceptionally bright, fluorescent dendrimers have been synthesized by using automated solid-state synthesis and phosphoramidite chemistry, thus opening potential alternatives for highly fluorescent probes for biological applications.^[21] Thinning of the reactive sites on the solid support was found to be crucial

for efficient dendrimer growth, and multiplier phosphoramidites with long, flexible arms give the highest coupling efficiency. It was also confirmed that increased intramolecular fluorophore spacing results in brighter dendrimers.

The family of dendrimers discussed in this report demonstrates that a single dendrimer can achieve intensities ≥ 70 times brighter than that of high-quantum-yield fluorescein. Furthermore, dendrimers promise single-functionalization points at the root, a unique property that QDs and fluorescent nanoparticles do not have. Therefore, this class of fluorescent dendrimers will be continuously optimized, aiming for small hydrodynamic radius, narrow polydispersity, and limited scattering profiles for ultra-bright molecular probes.

Experimental Section

Dendrimer syntheses

Dendrimers **D1–D8** were synthesized by using an 8909 Expedite Nucleic Acid Synthesis System. All reagents were freshly prepared except for tetrazole activator solution, which was purchased from Fisher Scientific. The solid supports or controlled pore glass (CPG) columns were purchased from Glen Research at the 0.2 μmol scale with 500 Å, 1000 Å, or 2000 Å pore sizes. Chromophoric phosphoramidites (**F2**, **F3**), spacer phosphoramidite (**S1**, **S2**), and multiplier phosphoramidite (**M1**, **M2**, **M3**, **M4**) with DMTr-protected hydroxyl groups for the chain growth were dissolved in CH_2Cl_2 at 60 mm. A custom coupling protocol for the phosphoramidite reagents was used in order to obtain the reported high yields.^[10b,22] Dendrimer growth on the CPG was either starting from a standard 3'-DNA base (A, T, C, or G) or a 3'-amino modifier (no DNA bases attached to the final dendrimers). When required, oligo DNA sequences were attached to either the dendrimer root or its dendrites or both. Once a spacer or dye was incorporated into the growing chain, deprotection removed the trityl group, which revealed the coupling yield from the previous step. Typically, the coupling yields range from 95–100%. Similarly, the incorporation of the dendritic unit reported an average yield of 92%. The duration of the solid-phase synthesis ranged from 160 s to 500 s depending on the activity of the phosphoramidites. Repeating such phosphoramidite coupling cycles produces 1st, 2nd, 3rd, 4th, and 8th generation dendrimers (**D1–D8**).

Trityl monitoring

One advantage of the phosphoramidite approach is that trityl monitoring allows facile reporting of the reaction yield for each generation. On the 8909 synthesizer, the built-in flow-through trityl monitor provides qualitative monitoring of step-wise synthesis. More importantly, the flow-through detector provides a non-linear response owing to detector saturation from order-of-magnitude concentration changes during dendrimer growth, as shown for dendrimer **D9** in Figure 1. Additionally, some phosphoramidites de-tritylate react faster than others, resulting in concentration spikes and thus response fluctuations of up to 20% for identical trityl concentrations. However, manually collecting and measuring the absorbance from the trityl byproduct after each step allows quantitative yield determination, as depicted in Figure 1 for dendrimer **D9**. Upon calibration to the manual trityl yields, it is apparent the flow-through detector displays a quasi-logarithmic response. The trityl yield decreases for the first three "thinning" steps, whereas a PEG spacer provides a stable trityl yield. The trityl response, how-

ever, jumps nearly 300% with the addition of the first trebler, followed by stable response for addition of another PEG spacer. This trend continues for four generations, so that the final trityl response is higher than the initial response from the dC CPG column. The response increases by $\sim 275\%$ (300% ideal) for each trebling step, and remains near 100% for nondendritic coupling. Similar exponential growth continues even up to the 8th generation in the synthesis of **D8**.

CPG size, coupling time, and scale

All dendrimers (summarized in Table 1) were synthesized at the 0.2 μmol scale by using CPG pore sizes of 500, 1000, or 2000 Å. Dendrimer growth efficiency did not seem to correlate with CPG pore size for low generation dendrimers ($G=1-3$), whereas the highest generation dendrimers ($G=4$ or 8) were only synthesized using 2000 Å pores. Repeated, extended coupling times were necessary to maximize coupling yields of nonstandard phosphoramidites. Thus, sub-100% coupling is attributed mostly to steric hindrance of crowded reactive groups.

Dendrimer purification

All dendrimers were deprotected by using concentrated $\text{NH}_4\text{OH}_{(\text{aq})}$, which simultaneously cleaved the dendrimer from the CPG support, removed the cyanoethoxy and 3'-amino Fmoc (9-fluorenylmethoxycarbonyl) protecting groups, and removed any DNA base protecting groups. Dendrimers were synthesized in either DMTr-On or DMTr-Off mode. The DMTr-Off dendrimers were desalted by using standard reverse phase C_8 oligomer purification columns (OPCs), easily removing unwanted salts and protecting group residues, whereas DMTr-On dendrimers were purified by using the standard OPC purification protocol, which additionally removes capped PEG chains owing to thinning. Even if coupling yields of 95–98% are achieved, the resulting hyperbranched polymer mixture will still exhibit relatively low polydispersity and uniformly bright single-molecule fluorescence.

Single-molecule spectroscopy

Single-molecule microscopy and spectroscopy were used to measure dendrimer brightness and photostability. The aqueous dendrimers were first spin-coated onto a cover slip in order to allow consistent CCD bright-field measurement of immobilized dendrimers as well as APD raster-scan images and time-trace analysis of diffraction-limited spots. Representative $10 \times 10 \mu\text{m}$ CCD images were collected with 2-second integration time for dendrimers **D1–D8** and compared with fluorescein and monomer **1e** (see the Supporting Information, Scheme S1). Statistical fluorescence histograms are provided in Figure 4. The monomers and the first-generation dendrimer, **D1**, are not much brighter than inorganic fluorescent impurities within the cover slip or other organic surface impurities. However, for the second-generation dendrimer, **D2**, and higher, there is a measurable increase in molecular brightness and signal-to-noise ratio (SNR), with the fourth-generation dendrimer, **D7**, and eighth-generation dendrimer, **D8**, being exceptionally bright. The zoomed-in $1 \times 1 \mu\text{m}$ CCD images of individual emitters from the same samples demonstrate that these emitters have diffraction-limited spots.

Acknowledgements

We acknowledge the support of the National Science Foundation (CHE-1212429).

Keywords: dendrimers · fluorescence · nanoprobcs · phosphoramidite · solid-phase synthesis

- [1] V. J. Pugh, Q. S. Hu, L. Pu, *Angew. Chem.* **2000**, *112*, 3784–3787; *Angew. Chem. Int. Ed.* **2000**, *39*, 3638–3641.
- [2] C. Kojima, B. Turkbey, M. Ogawa, M. Bernardo, C. A. S. Regino, L. H. Bryant, P. L. Choyke, K. Kono, H. Kobayashi, *Nanomedicine* **2011**, *7*, 1001–1008.
- [3] a) D. Luo, K. Haverstick, N. Belcheva, E. Han, W. M. Saltzman, *Macromolecules* **2002**, *35*, 3456–3462; b) Y. J. Tsai, C. C. Hu, C. C. Chu, I. Toyoko, *Biomacromolecules* **2011**, *12*, 4283–4290.
- [4] a) Y. E. Kurtoglu, R. S. Navath, B. Wang, S. Kannan, R. Romero, R. M. Kannan, *Biomaterials* **2009**, *30*, 2112–2121; b) L. Albertazzi, B. Storti, L. Marchetti, F. Beltram, *J. Am. Chem. Soc.* **2010**, *132*, 18158–18167.
- [5] A. Arakaki, K. Shibata, T. Mogi, M. Hosokawa, K. Hatakeyama, H. Gomyo, T. Taguchi, H. Wake, T. Tanaami, T. Matsunaga, T. Tanaka, *Polym. J.* **2012**, *44*, 672–677.
- [6] a) D. J. Liu, S. De Feyter, M. Cotlet, A. Stefan, U. M. Wiesler, A. Herrmann, D. Grebel-Koehler, J. Q. Qu, K. Mullen, F. C. De Schryver, *Macromolecules* **2003**, *36*, 5918–5925; b) T. Weil, U. M. Wiesler, A. Herrmann, R. Bauer, J. Hofkens, F. C. De Schryver, K. Mullen, *J. Am. Chem. Soc.* **2001**, *123*, 8101–8108; c) D. J. Liu, S. De Feyter, M. Cotlet, U. M. Wiesler, T. Weil, A. Herrmann, K. Mullen, F. C. De Schryver, *Macromolecules* **2003**, *36*, 8489–8498; d) J. M. J. Frechet, *Proc. Natl. Acad. Sci. USA* **2002**, *99*, 4782–4787.
- [7] a) I. Oesterling, K. Mullen, *J. Am. Chem. Soc.* **2007**, *129*, 4595–4605; b) M. Cotlet, T. Vosch, S. Habuchi, T. Weil, K. Mullen, J. Hofkens, F. C. De Schryver, *J. Am. Chem. Soc.* **2005**, *127*, 9760–9768.
- [8] C. Minard-Basquin, T. Weil, A. Hohner, J. O. Radler, K. Mullen, *J. Am. Chem. Soc.* **2003**, *125*, 5832–5838.
- [9] D. Görl, X. Zhang, F. Würthner, *Angew. Chem.* **2012**, *124*, 6434–6455; *Angew. Chem. Int. Ed.* **2012**, *51*, 6328–6348.
- [10] a) A. D. Shaller, W. Wang, H. Y. Gan, A. D. Q. Li, *Angew. Chem.* **2008**, *120*, 7819–7823; *Angew. Chem. Int. Ed.* **2008**, *47*, 7705–7709; b) W. Wang, W. Wan, H. H. Zhou, S. Q. Niu, A. D. Q. Li, *J. Am. Chem. Soc.* **2003**, *125*, 5248–5249; c) W. Wang, L. S. Li, G. Helms, H. H. Zhou, A. D. Q. Li, *J. Am. Chem. Soc.* **2003**, *125*, 1120–1121.
- [11] a) S. K. Yang, X. H. Shi, S. Park, S. Doganay, T. Ha, S. C. Zimmerman, *J. Am. Chem. Soc.* **2011**, *133*, 9964–9967; b) T. Heek, C. Fasting, C. Rest, X. Zhang, F. Würthner, R. Haag, *Chem. Commun.* **2010**, *46*, 1884–1886; c) B. X. Gao, H. X. Li, H. M. Liu, L. C. Zhang, Q. Q. Bai, X. W. Ba, *Chem. Commun.* **2011**, *47*, 3894–3896.
- [12] a) C. Kohl, T. Weil, J. Q. Qu, K. Mullen, *Chem. Eur. J.* **2004**, *10*, 5297–5310; b) J. Q. Qu, C. Kohl, M. Pottek, K. Mullen, *Angew. Chem.* **2004**, *116*, 1554–1557; *Angew. Chem. Int. Ed.* **2004**, *43*, 1528–1531; c) R. O. Marcon, J. G. dos Santos, K. M. Figueiredo, S. Brochsztein, *Langmuir* **2006**, *22*, 1680–1687; d) F. Yukruk, A. L. Dogan, H. Canpinar, D. Guc, E. U. Akkaya, *Org. Lett.* **2005**, *7*, 2885–2887.
- [13] D. Aigner, S. M. Borisov, I. Klimant, *Anal. Bioanal. Chem.* **2011**, *400*, 2475–2485.
- [14] M. S. Shchepinov, I. A. Udaloova, A. J. Bridgman, E. M. Southern, *Nucleic Acids Res.* **1997**, *25*, 4447–4454.
- [15] a) J. S. Klos, J. U. Sommer, *Macromolecules* **2009**, *42*, 4878–4886; b) S. Zou, H. Schonherr, G. J. Vancso, *Angew. Chem.* **2005**, *117*, 978–981; *Angew. Chem. Int. Ed.* **2005**, *44*, 956–959.
- [16] a) X. Feng, D. Taton, R. Borsali, E. L. Chaikof, Y. Gnanou, *J. Am. Chem. Soc.* **2006**, *128*, 11551–11562; b) I. Willerich, H. Ritter, F. Grohn, *J. Phys. Chem. B* **2009**, *113*, 3339–3354.
- [17] a) J. J. Han, A. D. Shaller, W. Wang, A. D. Q. Li, *J. Am. Chem. Soc.* **2008**, *130*, 6974–6982; b) J. J. Han, W. Wang, A. D. Q. Li, *J. Am. Chem. Soc.* **2006**, *128*, 672–673; c) D. H. Hu, Z. Y. Tian, W. W. Wu, W. Wan, A. D. Q. Li, *J. Am. Chem. Soc.* **2008**, *130*, 15279.
- [18] a) W. C. W. Chan, S. M. Nie, *Science* **1998**, *281*, 2016–2018; b) M. Bruchez Jr., M. Moronne, P. Gin, S. Weiss, A. P. Alivisatos, *Science* **1998**, *281*, 2013–2016.
- [19] a) S. Masuo, T. Vosch, M. Cotlet, P. Tinnefeld, S. Habuchi, T. D. M. Bell, I. Oesterling, D. Beljonne, B. Champagne, K. Mullen, M. Sauer, J. Hofkens, F. C. De Schryver, *J. Phys. Chem. B* **2004**, *108*, 16686–16696; b) F. C. De Schryver, T. Vosch, M. Cotlet, M. Van der Auweraer, K. Mullen, J. Hofkens, *Acc. Chem. Res.* **2005**, *38*, 514–522; c) P. Tinnefeld, K. D. Weston, T. Vosch, M. Cotlet, T. Weil, J. Hofkens, K. Mullen, F. C. De Schryver, M. Sauer, *J. Am. Chem. Soc.* **2002**, *124*, 14310–14311.
- [20] Z. Tian, A. D. Shaller, A. D. Q. Li, *Chem. Commun.* **2009**, 180–182.
- [21] Z. Y. Tian, A. D. Q. Li, *Acc. Chem. Res.* **2013**, *46*, 269–279.
- [22] W. Wang, A. D. Q. Li, *Bioconjugate Chem.* **2007**, *18*, 1036–1052.

Received: May 7, 2014

Published online on August 8, 2014